Physica C 471 (2011) 625–629

Contents lists available at ScienceDirect

Physica C

journal homepage: www.elsevier.com/locate/physc

Hall effect of FeTe and Fe($Se_{1-x}Te_x$) thin films

I. Tsukada [a,c,*], M. Hanawa [a,c], Seiki Komiya [a,c], A. Ichinose [a,c], T. Akiike [b,c], Y. Imai [b,c], A. Maeda [b,c]

[a] Central Research Institute of Electric Power Industry, 2-6-1 Nagasaka, Yokosuka, Kanagawa 240-0196, Japan
[b] Department of Basic Science, The University of Tokyo, 3-8-1 Komaba, Meguro, Tokyo 153-8902, Japan
[c] Japan Science and Technology Agency, 5 Sanbancho, Chiyoda, Tokyo 102-0075, Japan

ARTICLE INFO

Article history:
Available online 12 May 2011

Keywords:
Iron chalcogenide superconductor
FeTe
Hall effect
Two-band model

ABSTRACT

The Hall effect is investigated in thin-film samples of iron–chalcogenide superconductors in detail. The Hall coefficient (R_H) of FeTe and Fe($Se_{1-x}Te_x$) exhibits a similar positive value around 300 K, indicating that the high-temperature normal state is dominated by hole-channel transport. FeTe exhibits a sign reversal from positive to negative across the transition to the low-temperature antiferromagnetic state, indicating the occurrence of drastic reconstruction in the band structure. The mobility analysis using the carrier density theoretically calculated reveals that the mobility of holes is strongly suppressed to zero, and hence the electric transport looks to be dominated by electrons. The Se substitution to Te suppresses the antiferromagnetic long-range order and induces superconductivity instead. The similar mobility analysis for Fe($Se_{0.4}Te_{0.6}$) and Fe($Se_{0.5}Te_{0.5}$) thin films shows that the mobility of electrons increases with decreasing temperature even in the paramagnetic state, and keeps sufficiently high values down to the superconducting transition temperature. From the comparison between FeTe and Fe($Se_{1-x}Te_x$), it is suggested that the coexistence of 'itinerant' carriers both in electron and hole channels is indispensable for the occurrence of superconductivity.

1. Introduction

New iron-based superconductors have attracted much attention since LaFeAs($O_{1-x}F_x$) was reported to show superconductivity at T = 26 K [1]. The highest T_c ever reported reaches 56 K [2], and still great efforts have been made to raise their T_c's. Iron–chalcogenide superconductors have the simplest structure among all the iron-based superconductors, and consist of only Fe and *Ch* (*Ch* = S, Se, and Te) [3,4]. There is a similarity in the crystallographic structure of Fe-*Ch* layer to that of Fe-*Pn* (*Pn* = As and P) layer implying a similar electronic state in both iron–pnictide and iron–chalcogenide superconductors. Indeed, the band calculation [5,6] predicted that there are five bands mainly originated from five 3*d* levels of Fe crossing the Fermi level to form Fermi surface.

However, these two compounds have several intrinsic differences. In Fe*Pn*, explicit carrier doping is possible by chemical substitution by elements with a different valence, and a rigid-band picture properly explains the evolution of electronic states by carrier doping. In Fe*Ch*, however, superconductivity is induced by isovalent substitution of Se and/or S to Te in FeTe, which suggests that the rigid-band picture no longer works. Thus the evolution of electronic states from parent antiferromagnetic to doped superconducting states might be more complicated than Fe*Pn* superconductors, and hence the electric-transport measurements, especially Hall measurements, using high-quality single-crystalline samples are indispensable for understanding the evolution of electronic states in Fe*Ch*.

In this paper, we present the detailed results on a comparative study of Hall measurements in both parent antiferromagnet FeTe, and superconducting Fe($Se_{1-x}Te_x$). We apply a semi-classical two-band Drude model and perform a phenomenological analysis of resistivity (ρ) and Hall coefficient (R_H) as functions not only of temperature but also of magnetic field. With the aid of carrier densities theoretically calculated for FeTe, we evaluate a mobility of electrons and holes, and discuss the key factor for the occurrence of superconductivity.

2. Experimental

Table 1 shows the sample specification. All the thin films were prepared by pulsed laser deposition method from carefully prepared polycrystalline target. Details are described elsewhere [7,8]. We have selected several substrate materials suitable for thin-film growth of iron chalcogenide superconductors. In the present study, all the films are grown on MgO (1 0 0) or $LaAlO_3$ (1 0 0), which have been already confirmed to be appropriate for growing Fe($Se_{1-x}Te_x$) [8]. We show the data of seven thin films: two FeTe, two Fe($Se_{0.4}Te_{0.6}$), and three Fe($Se_{0.5}Te_{0.5}$) thin films.

* Corresponding author. Address: Materials Science Research Laboratory, 2-6-1 Nagasaka, Yokosuka, Kanagawa 240-0196, Japan. Tel.: +81 46 856 2121; fax: +81 46 856 5571.
E-mail address: ichiro@criepi.denken.or.jp (I. Tsukada).

0921-4534/$ - see front matter © 2011 Elsevier B.V. All rights reserved.
doi:10.1016/j.physc.2011.05.012

Table 1
Sample specifications.

Composition	Name	Substrate	c (Å)	Thickness (nm)	T_{c0} (K)
FeTe	FeTe-1	MgO (1 0 0)	6.285	165	–
FeTe	FeTe-2	$LaAlO_3$ (1 0 0)	6.275	165	–
$Fe(Se_{0.4}Te_{0.6})$	S40T60-1	MgO (1 0 0)	5.891	11	6.0
$Fe(Se_{0.4}Te_{0.6})$	S40T60-2	$LaAlO_3$ (1 0 0)	5.910	11	5.6
$Fe(Se_{0.5}Te_{0.5})$	S50T50-1	MgO (1 0 0)	5.904	200	10.0
$Fe(Se_{0.5}Te_{0.5})$	S50T50-2	$LaAlO_3$ (1 0 0)	5.901	210	11.4
$Fe(Se_{0.5}Te_{0.5})$	S50T50-3	$LaAlO_3$ (1 0 0)	–	90	3.4

One may notice that two $Fe(Se_{0.4}Te_{0.6})$ films are very thin (11 nm), but their c-axis length are close to those reported for polycrystalline sample as those of the other relatively thick films are [9], and thus we expect no significant difference caused by the film thickness. We used a metal mask to make the film in a six-terminal shape as shown in Fig. 1 in order not only to measure Hall resistance precisely but also to measure the thickness using a stylus profiler [10]. Longitudinal and transverse resistivities are measured using Physical Properties Measurement System (PPMS) under the magnetic field up to $\mu_0 H = 13$ T.

3. Results and discussion

3.1. X-ray diffraction and transmission electron microscopy

Fig. 2a shows X-ray diffractions of FeTe films. All the films have highly c-axis oriented structure. The calculated c-axis lengths are summarized in Table 1. In both cases (MgO and $LaAlO_3$ substrates), the c-axis lengths of the films are comparable to that of $Fe_{1.07}Te$ bulk crystal. This suggests that the films do not feel tensile stress in contrast to what is reported by Han et al. [11]. It should be also noted that the c-axis length is not so much different between the films on MgO and $LaAlO_3$, which is a similar result to what was observed in $Fe(Se_{0.5}Te_{0.5})$ thin films [8]. The substitution of Se shrinks the c axis as shown in Fig. 2b and c. $Fe(Se_{0.4}Te_{0.6})$ and $Fe(Se_{0.5}Te_{0.5})$ films show the shorter c-axis length than FeTe. However, in our experiments, we did not see an explicit correlation of the chemical composition and the c-axis length between these two compounds.

Fig. 3a and b show cross sectional images of FeTe and $Fe(Se_{0.5}Te_{0.5})$ thin films. In our previous report, we have revealed that the diffusion of oxygen to the grown film becomes significant on some substrate materials, such as YSZ and $LaSrGaO_4$. On MgO and $LaAlO_3$ substrates, however, the interface is quite sharp and no trace of oxygen diffusion is observed in both FeTe and $Fe(Se_{0.5}Te_{0.5})$ thin films. This property is quite beneficial for better in-plane orientation of the grown films. On both substrates, we always obtain MgO [1 0 0] || Fe*Ch* [1 0 0] and $LaAlO_3$ [1 0 0] || Fe*Ch* [1 0 0] as was also confirmed by X-ray diffraction, while on other substrates we frequently observe domains that have different in-plane orientations [8]. Therefore, we use MgO (1 0 0) and $LaAlO_3$ (1 0 0) for FeTe and $Fe(Se_{1-x}Te_x)$ whenever we need to grow a 'single-crystalline' Fe*Ch* thin films.

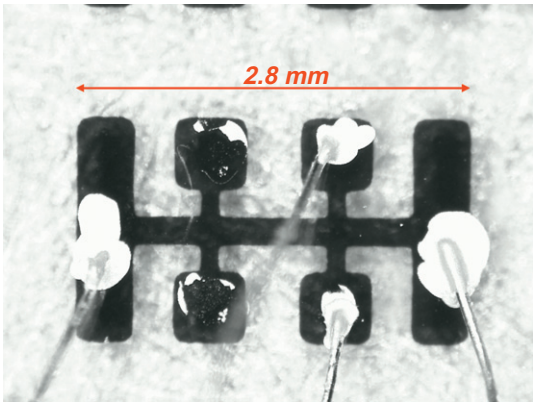

Fig. 1. Photograph of six-terminal shape sample (FeTe-1). The Au-wire leads of this particular configuration are for Hall-effect measurements.

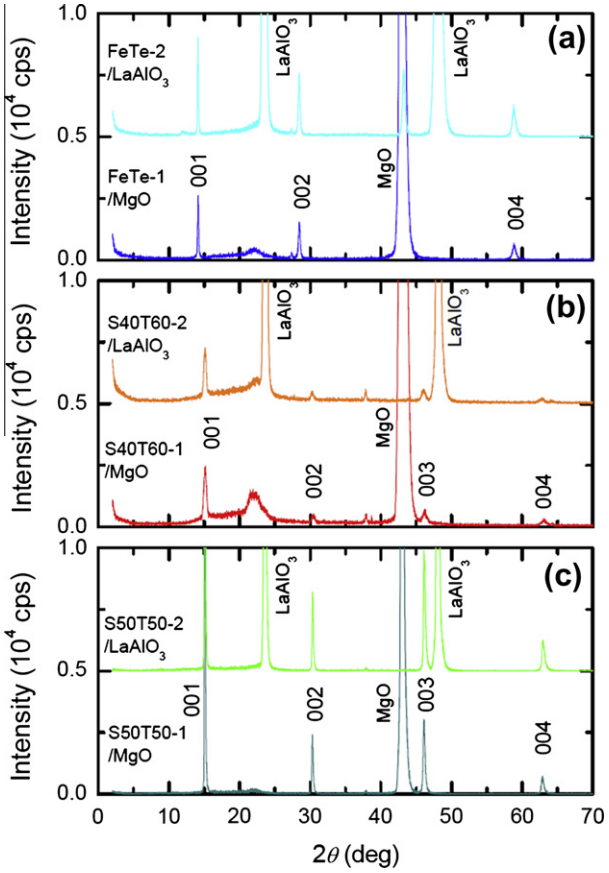

Fig. 2. X-ray diffraction of (a) FeTe thin films on MgO (1 0 0) and $LaAlO_3$ (1 0 0), (b) $Fe(Se_{0.4}Te_{0.6})$ thin films on MgO (1 0 0) and $LaAlO_3$ (1 0 0), (c) $Fe(Se_{0.5}Te_{0.5})$ thin films on MgO (1 0 0) and $LaAlO_3$ (1 0 0).

3.2. Resistivity

The temperature dependence of resistivity is summarized in Fig. 4. Let us first see the data of FeTe. The magnitude of resistivity is as low as that reported for bulk single crystals in both the films, while the details are different from the bulk crystals [12–14]. The most remarkable difference is the absence of discontinuous jump in ρ indicating that a sharp first-order tetragonal-to-monoclinic structural transition does not occurs in these films. Instead a broad peak appears around 80 K, which may be due to the influence of epitaxy with the substrate. However, the resistivity behavior below 80 K is roughly the same as that of bulk crystals, and we may infer the antiferromagnetic long-range order evolves in the low-temperature phase.

$Fe(Se_{0.4}Te_{0.6})$ and $Fe(Se_{0.5}Te_{0.5})$ show superconductivity. The T_c of S40T60-1 is 6.0 K, while that of S50T50-2 reaches 11.4 K, which is the highest T_c ever observed in our films. In both cases, we did not observe a significant influence of substrate materials to the resistivities. All the films show a similar T-dependence at relatively